



Effect of topographic slope on the export of nitrate in humid catchments

Jie Yang¹, Ingo Heidbüchel^{2, 4}, Chunhui Lu¹, Yueqing Xie³, Andreas Musolff², and Jan H. Fleckenstein^{2, 4}

- 5 ¹State Key Laboratory of Hydrology-Water Resources and Hydraulic Engineering, Hohai University, Nanjing, China
²UFZ - Helmholtz-Centre for Environmental Research GmbH, Department of Hydrogeology, Leipzig, Germany
³School of Earth Sciences and Engineering, University of Nanjing, Nanjing, China
⁴Hydrologic Modeling Unit, Bayreuth Center of Ecology and Environmental Research (BayCEER), University of Bayreuth, Bayreuth, Germany

10

Correspondence to: Jie Yang (yangj@hhu.edu.cn)

Key Points

- 15 • Topographic slope affects in-stream nitrate concentrations in a three-class pattern rather than being exclusively monotonous
- Young streamflow fraction and nitrate concentration decrease sharply once flatter landscapes are not able to maintain fast preferential overland flow paths
- The seasonal fluctuation of in-stream concentration is caused mainly by the temporal variability of nitrate degradation for catchments in temperate humid climates
- 20 • Seasonal fluctuations tend to be more pronounced in flatter landscapes.

Abstract. Excess export of nitrate to streams affects ecosystem structure and functions and has been an environmental issue attracting world-wide attention. The dynamics of catchment-scale solute export from diffuse nitrate sources can be explained by the activation and deactivation of dominant flow paths, as solute attenuation (including the degradation of nitrate) is linked to the age composition of outflow. Previous data driven studies suggested that catchment topographic slope has strong impacts on the age composition of streamflow and consequently on in-stream solute concentrations. However, the impacts have not been systematically assessed in terms of solute concentration levels and variation, particularly in humid catchments with strong seasonality in meteorological forcing. To fill this gap, we modeled the groundwater flow and nitrate transport for a cross-section of a small agricultural catchment in Central Germany. We used the fully coupled surface and subsurface numerical simulator HydroGeoSphere to model groundwater and overland flow as well as nitrate concentrations. We computed the water ages using numerical tracer experiments. To represent various topographic slopes, we additionally simulated ten synthetic cross-sections generated by modifying the mean slope from the real-world scenario while preserving the land surface micro-topography. Results suggest a three-class response of in-stream nitrate concentrations to topographic slope, from class 1 (slope >

25
30



35 1:60), via class 2 ($1:100 < \text{slope} < 1:60$), to class 3 ($\text{slope} < 1:100$). Flatter landscapes tend to produce higher in-stream
nitrate concentrations within class 1 or class 3, however, not within class 2. Young streamflow fractions and nitrate
concentrations decrease sharply when flatter landscapes are not able to maintain fast preferential discharge paths (e.g.
seepage). The variation of in-stream concentrations, controlled by degradation variability rather than by nitrate source
variability, shows a similar three-class response. Our results improve the understanding of nitrate export in response
40 to topographic slope in temperate humid climates, with important implications for the management of stream water
quality.

Keywords: topographic slope, coupled surface-subsurface model, young streamflow, in-stream nitrate,
HydroGeoSphere

45

1 Introduction

Globally nearly 40% of land is used for agricultural activities [Foley *et al.*, 2005], which constitutes the major source
of pollution with nutrients such as nitrate (referred as to N-NO_3 in this study). Excess export of nitrate to streams
threatens ecosystem structure and functions, as well as human health via drinking water [Vitousek *et al.*, 2009; Alvarez-
50 Cobelas *et al.*, 2008; Dupas *et al.*, 2017]. This has been an environmental issue attracting attention in Germany and
world-wide. The dynamics of nitrate export from diffuse sources are regulated by the dominant flow paths that
determine the speed at which precipitation travels through catchments before it reaches the stream [Jasechko *et al.*
2016]. The process is subject to both hydrological and biogeochemical influences mediated by various factors (e.g.
catchment topography, aquifer properties, redox boundaries). From the perspective of sustainable intensification,
55 process understanding and assessment of potential effects of catchment topography on nitrate export are critical for
the management of water quality in connection with agricultural activity.

Field observations in central German catchments indicate that in-stream nitrate concentrations (C_Q) are generally
higher at downstream areas with gentle topography compared to more mountainous upstream areas [Dupas *et al.*,
2017]. This provides strong evidence that catchment topographic slope can influence the nitrate export. In terms of
60 water age analyses, Jasechko *et al.* [2016] using oxygen isotope data from 254 watersheds worldwide showed
significant negative correlation between the young (age < 3 months) streamflow fraction and the mean topographic
gradient. They stated that young streamflow is more prevalent in flatter catchments as these catchments are
characterized by shallow lateral flow, while it is less prevalent in steeper mountainous catchments as these catchments
promote deep vertical infiltration. This statistically significant trend is consistent with the common finding that fast
65 shallow flow paths produce young discharge and potentially promote high in-stream solute concentrations [Böhlke *et al.*
2007; Benettin *et al.* 2015; Hrachowitz *et al.* 2016; Blaes *et al.* 2017]. However, apart from these data-driven
analyses, a more mechanistic examination/explanation with the aid of fully resolved flow paths is still required. Wilusz
et al. [2017] used a coupled rainfall-runoff and transit time model to investigate the young streamflow fraction, with
a focus on the effect of rainfall variability rather than on topography and solute export. The effect of topographic slope
70 on C_Q has not been subject to systematical testing.



Seasonal fluctuation of C_Q is commonplace in catchments under seasonal hydrodynamic forcing. Field observations in mountainous central German catchments indicate that nitrate concentrations, as well as the mass load, in streams vary seasonally, with maxima during the wet winter and minima during the dry summer [Dupas *et al.*, 2017]. Data-driven analyses by Musolff *et al.* [2015] and Dupas *et al.* [2017] suggested the systematic seasonal (de)activation of nitrate source zones as an explanation for such seasonal variability. Under wetter winter conditions the near-surface nitrate source zones in agricultural soils are connected to the stream by fast shallow flow paths. Under drier summer conditions those nitrate source zones are deactivated because their direct hydrologic connectivity to the stream is replaced with deeper flow paths [Dupas *et al.*, 2017]. Based on high-frequency monitoring in the Wood Brook catchment in the UK, Blaen *et al.* [2017] also reported mobilization of nitrate from the uppermost soil layers during high flow conditions via shallow preferential flow paths, which would not occur during base flow in drier periods. This behavior leads to a seasonally-variable nitrate loading due to changing flow paths and the associated variation in transit time that has been observed in many catchments [Benettin *et al.*, 2015; Hrachowitz *et al.*, 2016; Kaandorp *et al.*, 2018; Rodriguez *et al.*, 2018; Yang *et al.* 2018]. However, how this fluctuation behaves in response to catchment land surface topography has not been assessed systematically yet. Such an assessment could improve our understanding of nitrate export from catchments of different topographic slopes not only in terms of the mean concentration but also regarding its seasonal variability.

Given that most of the above studies used data driven analysis, numerical modeling is an effective tool for the analysis of water flow, age and solute transport, eliminating the need for large amounts of field data. Physically-based hydrogeological models (like, e.g., HydroGeoSphere [Therrien *et al.*, 2010]) resolve the spatially-explicit details within a catchment including the full variability of 3D flow paths in the subsurface, helping to understand the seasonally changing flow patterns in response to different catchment topographies. Additionally, the widely used fully-coupled surface-subsurface technology simulates the catchment as an integrated system, providing details of surface water-groundwater exchanges fluxes. These details help to identify paths of rapid discharge to the land surface that can considerably improve the interpretation of nitrate-export patterns.

Transit time distributions (TTDs) have been widely used to interpret hydrological and chemical responses in catchment outfluxes – both in discharge (Q) and in evapotranspiration (ET) [van der Velde *et al.*, 2012; Rinaldo *et al.* 2015; Harman *et al.*, 2015; 2019]. They characterize how a catchment stores, mixes and releases water as well as dissolved solutes at large spatial and temporal scales [Benettin *et al.*, 2015; Harman, 2015; van der Velde *et al.*, 2010, 2012; Hrachowitz *et al.*, 2015; Van Meter *et al.*, 2017]. Given that the nitrate attenuation is linked to the age composition of outflow, the TTDs are ideal tools for interpreting the concentration dynamics with regard to catchment topographic slope. Estimating water ages in natural catchments is still a challenge due to varying climate conditions, as well as the errors in algorithms (e.g. errors in the flow field during particle tracking) and limited computational capacity. Yang *et al.* [2018] used particle tracking to compute the age distributions in the subsurface of a study catchment (while omitting the 4% of total discharge produced by direct surface runoff and ignoring the frequent exchange fluxes that may be important for solute export due to their short transit times). In this study we determine the age compositions of Q and ET using numerical tracer experiments, where advective-dispersive transport of the tracers was solved using the fully-coupled surface-subsurface framework of HydroGeoSphere. The computed age dynamics based on the tracer



concentrations were representative as the tracers were able to track all the flow processes such as surface runoff, groundwater flow and surface-subsurface interaction.

110 In this study, we attempted to systematically assess the effect of catchment topographic slopes on the nitrate export
dynamics in terms of the concentration level and its seasonal variability. We also seek mechanical explanations for
the previously found behaviors from data-driven studies (like, e.g., *Jasechko et al.* [2016]) with the help of fully
resolved flow paths. First, we chose a real-world cross-section from the small agricultural catchment ‘Schäfertal’ in
Central Germany, which is characterized by strong seasonality in hydrodynamic forcing with associated shifts in the
115 dominant flow paths [*Yang et al.*, 2018]. This catchment is typical for many catchments with hilly topography under
a temperate humid climate. We created eleven model scenarios by adjusting the mean slope of the real-world cross-
section while preserving the land surface micro-topography and aquifer heterogeneity. Next, we modeled the water
flow and nitrate transport for each cross-section. The flow and transport were solved using the fully coupled surface
and subsurface numerical simulator HydroGeoSphere, and the water ages were computed using numerical tracer
120 experiments. Finally, the modeled flowpaths, water ages and nitrate concentrations under various topographic slopes
were analyzed. Through this study, we aimed to (1) examine the relationship between topographic slope and C_Q , and
to (2) assess the seasonal variation of C_Q and its controls regarding different topographic slopes. The results were
supposed to improve the understanding of the effects of certain catchment characteristics on nitrate export dynamics
with potential implications for the management of stream water quality and agricultural activity.

125

2 Data collection

2.1 Real-world and synthetic cross-sections

Our study was conducted on a vertical cross-section selected from the catchment ‘Schäfertal’. This catchment is
situated in the lower part of the Harz Mountains, Central Germany (Figure 2a). The catchment has an area of 1.44
130 km². The hillslopes are mostly used for intensive agriculture while the valley bottom contains riparian zones with
pasture and a small stream draining the water out of the catchment. The gauging station at the outlet of the catchment
provides Q records. This gauging station is the only outlet for discharging water from the catchment, because a
subsurface wall was erected underneath the gauging station across the valley to block subsurface flow out of the
catchment. A meteorological station 200 m from the catchment outlet provides records of precipitation (J), air and soil
135 temperatures, radiation and wind speed. The modeled cross-section is perpendicular to the stream with a length of 420
m (Figure 2a, b) and a mean topographic slope of 1:20. The aquifer thickness varies from ~5 m near the valley bottom
to ~2 m at the top of the hillslope. Groundwater storage is low (~500 mm) in such a thin aquifer and mostly limited to
the vicinity of the channel with the upper part of the hillslopes generally unsaturated. The stream bed has a depth of
1.5 m below the land surface, prescribed on the valley side of the cross-section. Aquifer properties (e.g. hydraulic
140 conductivity) change from the hillslope, dominated by Luvisols and Cambisols, to the valley bottom, dominated by
Gleysols and Luvisols [*Anis and Rode*, 2015]. Apart from that, the aquifer generally consists of two layers: the top
layer of approximately 0.5 m thickness with higher porosity and a developed root zone from crops, and the base layer



with smaller porosity due to high loam content [Yang *et al.*, 2018]. Subsequently, six property zones were used (Figure 1b), with zonal parameter values following the model in Yang *et al.*, [2018] listed in Table 1.

145 Based on this real-world cross-sectional aquifer, ten synthetic cross-sections were generated by adjusting the mean topographic slope from 1:20 (steep) to 1:22, 1:25, 1:30, 1:40, 1:60, 1:80, 1:100, 1:200, 1:500 and 1:1000 (flat), while preserving the land surface micro-topography, aquifer depth and heterogeneity (Figure 1b). In total, eleven cross-sections were used for flow and transport simulations.

150 2.2 Climates

The considered climate for the cross-sections was derived from the catchment ‘Schäfertal’ located in a region with temperate humid climate and pronounced seasonality. According to the meteorological data records from 1997 to 2007, the mean annual J and Q (per unit area) are 610 mm and 160 mm, respectively. Actual mean annual ET based on the ten-year water balance ($J = ET + Q$) is 450 mm. Mean annual potential ET is 630 mm [Yang *et al.*, 2018]. The humid climate is representative for wet regions, quantified by an aridity index ($J / \text{potential ET}$ [Li *et al.*, 2019]) of 1.0. The ET is the main driver of the hydrologic seasonality as the precipitation is more uniformly distributed across the year (Figure 1c). To acknowledge this fact, we selected the data records of the year 2005, and calculated the annual J and monthly-averaged potential ET. Using these averaged values in the study can accelerate the simulations and simplify the analysis while preserving the main characteristics of the meteorological forcing to the system.

160

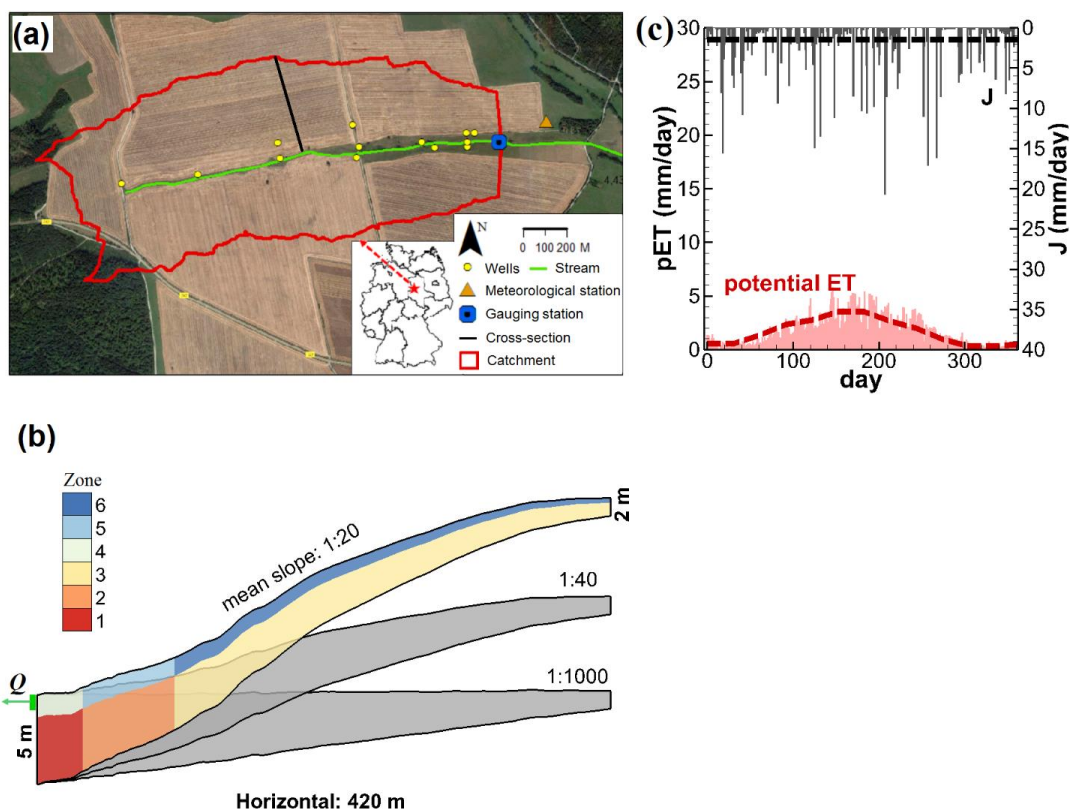


Figure 1. (a) The catchment ‘Schäfertal’, Central Germany (background image from © Google Maps). (b) The cross-sectional aquifer marked in (a) with a slope of 1:20 and two synthetic ones with topographic slopes of 1:40 and 1:1000. (c) The measured precipitation J and the estimated potential evapotranspiration ET for the humid climate [Yang *et al.*, 2018]. The dashed lines represent the annual (J) and monthly (ET) averages.

165

3 Methods

3.1 Flow and nitrate transport

It is necessary to solve both groundwater and surface water flow because the spatially-explicit details in the model catchment including the specific flow paths and exchange fluxes are necessary to interpret the effect of varying topographic slope on nitrate transport. We simulated the flow system using the fully coupled surface and subsurface numerical model HydroGeoSphere, which solves for variably saturated groundwater flow with the Richards’ equation and for surface flow with the diffusion-wave approximation of the Saint-Venant equations [Therrien *et al.*, 2010]. Additionally, the exchange flux between groundwater and surface water can be implicitly simulated. The nitrate transport is simulated in the groundwater flow, surface flow and exchanges fluxes by solving the advection-dispersion-diffusion equation describing the conservation of nitrate mass. The model has been successfully used to simulate

170

175



catchment hydrological processes and solute transport in many studies [e.g. Therrien et al., 2010; Yang et al., 2018], therefore governing equations and technical details are not explicitly repeated here.

180 The modeled subsurface of the cross-sections was discretized into 15 horizontal element-layers between land surface and aquifer base, with thinner layers in the upper part (~ 0.05 m) to better represent the unsaturated zone in more detail and thicker layers in the lower part (~ 1 m). The cross-sections were 420 m long and uniformly discretized into 200 cells. Apart from that, each cross-section had a width (lateral direction perpendicular to the cross-section) of 100 m discretized uniformly into 10 cells. The reason for that was to avoid boundary influences that may have been caused by the lateral flow boundary condition (described later). In total, the discretization led to 30,000 block elements for the surface. The topmost 2,000 rectangles (200×10) were used to discretize the surface domain, where surface flow was simulated.

Table 1. The key aquifer parameters and their values following Yang et al., [2018]. Zonal values are ordered from zone 1 to zone 6.

Parameter	Process	Type	Value
Hydraulic conductivity	Subsurface	zonal	2.00, 0.13, 1.18, 0.02, 0.02, 2.00 m day ⁻¹
Porosity	Subsurface	zonal	0.1, 0.1, 0.1, 0.35, 0.35, 0.35 [-]
Residual saturation	Subsurface	uniform	0.08 [-]
Inverse of air entry pressure α	Subsurface	uniform	3.6 m ⁻¹
Pore-size distribution index β	Subsurface	uniform	2 [-]
Manning roughness coefficient	Surface	uniform	6.34·10 ⁻⁶ day m ^{-1/3}
Longitudinal dispersivity	Transport	uniform	8 m
Lateral and vertical dispersivity	Transport	uniform	0.8 m
Molecular diffusion coefficient	Transport	uniform	10 ⁻⁹ m ² s ⁻¹
Degradation coefficient	Transport	uniform	0.009 day ⁻¹
Transpiration fitting parameters:			
C1	ET	uniform	0.17 [-]
C2	ET	uniform	0.00 [-]
C3	ET	uniform	3.00 [-]
Transpiration limiting saturations:			
Wilting point	ET	uniform	0.1 [-]
Field capacity	ET	uniform	0.2 [-]
Oxic limit	ET	uniform	0.9 [-]
Anoxic limit	ET	uniform	1.0 [-]
Evaporation limiting saturations:			
Minimum	ET	uniform	0.1 [-]
Maximum	ET	uniform	0.2 [-]

190



Parameters and boundary conditions for flow

The key model parameters for simulating groundwater flow, surface flow and ET are listed in Table 1. Their values
195 were taken from previous work [Yang *et al.*, 2018], where a hydrological flow model was built and calibrated against
measured groundwater levels and Q for the entire catchment. For each cross-section, constant J and time-variant
potential ET were applied to the aquifer top. HydroGeoSphere calculates actual ET from potential ET taking into
account the modeled water content, leaf area index and root depth distributions. A free-drainage boundary condition
was assigned to the topmost 1.5 m of the subsurface at the valley side (left side) boundary (Figure 1b), enabling
200 subsurface discharge to the channel. A critical depth boundary [Therrien *et al.*, 2010] was assigned to the left-side
edge of the land surface, allowing surface discharge to the channel. In the 3D catchment, surficial flowpaths can
connect the surface water ponding in the depressions of the land surface. In our 2D model, it is unrealistic to force
these surficial flowpaths to be parallel to the cross-section. Therefore, our model allowed for the lateral exit of surface
water via the depressions of the land surface by assigning critical depth boundary conditions there. This lateral exit
205 was also counted as surface discharge to the channel. Finally, the total discharge Q can be calculated by summarizing
the subsurface and surface discharge.

Parameters and boundary conditions for transport

The nitrogen pool in the soil is controlled by various complex processes. It is replenished by inputs from atmospheric
deposition, biological fixation, animal manure from the pasture area, and fertilizer from the farmland on the hillslopes.
210 Nitrate-N that can be transported with water is formed from this (organic) nitrogen pool by a microbiological
immobile-mobile exchange process [Musolff *et al.*, 2017; Van Meter *et al.*, 2017]. In our study, it is not necessary to
fully implement all the complexities of the different nitrogen pools and transformations into the model, because we
focus on the in-stream concentration responses with regard to catchment topography, rather than on the full nitrogen
cycle of the catchment. Therefore, we assumed that a nitrate source concentration C_j was associated with the
215 precipitation. The C_j , which is time-variant, comprehensively defines the amount of dissolved nitrate that can enter
the storage along with precipitation. In this study, the C_j curve followed the time-variant nitrate leaching
concentrations calculated by Nguyen *et al.*, [2021] using a mesoscale nitrate export model (Figure 2). Additionally,
we also considered cases with constant C_j which is the average of the time-variant values. This constant C_j was used
to quantify the source contribution to the variation of instream concentrations (described in section 3.3).
220 To simplify the transport processes, the nitrate transported with ET (representing plant-uptake) was assumed to not
alter the nitrate concentration of the water in storage, neglecting the evapoconcentration effect, because its potential
effect to cause source variability was implicitly considered by forcing the source concentration to vary along the C_j
curve. The denitrification in the system was described by the first order decay process with a degradation rate
coefficient λ of 0.009 day^{-1} according to Nguyen *et al.*, [2021] studying the area including the catchment Schifertal.
225 Longitudinal and transverse dispersivity values were 8 m and 0.8 m, respectively.

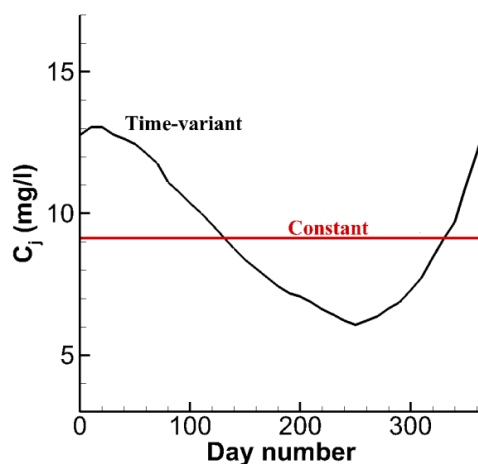


Figure 2. The variable and the constant nitrate source concentrations. The constant source is the annual average of
230 the variable source.

In total, we simulated the flow and transport for 22 scenarios (11 topographic slopes \times 2 for variable/constant nitrate
sources). For each scenario, the simulations were run for 100 years with identical boundary conditions for each year.
The first 99 years were used as a spin-up phase to assure a dynamic equilibrium (i.e. to achieve simulated variables,
such as heads and concentrations, being identical between years), and the last year was used for actual observation
235 and analysis. The CPU time of each simulation was \sim 4 hours.

3.2 Water ages

The water stored in a catchment (storage), Q and ET is characterized by its age distribution, as it comprises water
parcels of different age from precipitation events that occurred in the past. The age distributions need to be calculated
240 for each aforementioned scenario to assess the responses of water ages on catchment topographic slope. Our model
setup (with virtual cross-sections and identical climate for each year) allowed us to perform long-term numerical tracer
experiments and to extract the age distributions.

We assumed that inert tracers of uniform concentration existed in precipitation. The tracers were applied to the land
surface as a third-type (Cauchy) boundary condition and were subjected to transport modeling. Tracer can exit the
245 aquifer via the outfluxes Q and ET . We considered a period of 200 years for the tracer experiments, which was
sufficiently long to ensure convergence of the computed water ages. The 200 years period was partitioned into 2400
months Δt . A different tracer was used for each of the periods resulting in a total of 2400 distinct tracers. The injection
of tracer i started at the beginning of its associated period t_0^i and lasted throughout the period with the precipitation.
The advective-dispersive multi-solutes transport was simulated using HydroGeoSphere. The first 199 years of the
250 simulation period were used a spin-up phase to ensure a dynamic equilibrium of calculated ages, minimizing the



influence of the initial conditions. The last year was used for the actual observations and the computation of age distributions. Solving the transport of the 2400 tracers is computationally expensive. However, because the climate (flow boundary conditions) was identical for each year, the transport simulation was performed only for the first 12 tracers that covered the course of a year. Based on these results, the results for the other 2388 tracers were manually reproduced (e.g., by shifting the concentration breakthrough curves of the 12 tracers in time while maintaining the shapes).

For each tracer, the breakthrough curves of the mass-fluxes of Q and ET, as well as the mass in storage were reported. For a specific time t , the age distributions for Q/ET/storage were computed by calculating the mass fraction of each tracer using:

$$p_{Q/ET/S}(T, t) = \frac{M^i(t)}{\Delta t \sum M^i(t)}$$

where $p_Q(T, t)$, $p_{ET}(T, t)$ are the age distributions of Q, ET (equivalent to TTD), and $p_S(T, t)$ is the age distributions of water in storage (equivalent to the residence time distribution - RTD). $M^i(t)$ is the mass-flux of the tracer i in Q or ET, or the mass stored in catchment at time t , $\sum M^i(t)$ is the sum of $M^i(t)$ over all tracers. T is the age that equals $t - t_0^i$ for tracer i .

For each scenario, the CPU time of the tracer experiment was ~8 hours. Based on the age distributions, we calculated the mean discharge age $T_Q(t)$, which is equivalent to the mean discharge transit time (simply referred to as 'discharge age' in the following sections). We calculated the young water fraction in streamflow $YF_Q(t)$, which is the fraction of streamflow with an age younger than three months (also referred to as 'young streamflow fraction' [Jasechko *et al.* 2016]). Similarly, the ET age $T_{ET}(t)$ and the young water fraction in ET $YF_{ET}(t)$ can be calculated as well (more details are described in Text S1 of the supporting information). Their responses to a change in topographic slope were analyzed.

3.3 Assessment variables

The simulations of flow, nitrate transport and water age provided in-stream nitrate concentrations $C_Q(t)$, streamflow ages $T_Q(t)$ and young water fractions $YF(t)$ for each scenario. They all fluctuated seasonally over the course of a year. The temporal means and standard deviations σ of these variables can be calculated. The temporal variation in C_Q can potentially be split and attributed to (i) the variability in the nitrate source concentration, referred to as source contribution, and (ii) the variability created by degradation associated with variable transit times, referred to as degradation contribution. To understand which of these processes has the dominant effect on C_Q variability, we quantified the source contribution by calculating the relative change of σ for C_Q when C_j switches from being time-variant to being constant between separate model scenarios (see section 3.1), as:

$$\text{Source contribution} = 1 - \frac{\sigma(C_Q) \text{ under constant } C_j}{\sigma(C_Q) \text{ under variable } C_j}$$



285 The calculated source contribution ranges from 0 (degradation-dominated) to 100 % (source-dominated). Additionally,
the *Damköhler* number ($Da = \bar{T}_Q \cdot \lambda$, [Oldham *et al.*, 2013]), which is a dimensionless ratio between the discharge
age and the reaction time, can be calculated to indicate the interplay between the rate of degradation and the time-
scale of transport. $Da > 1$ indicates a faster degradation time than transport time and vice versa.

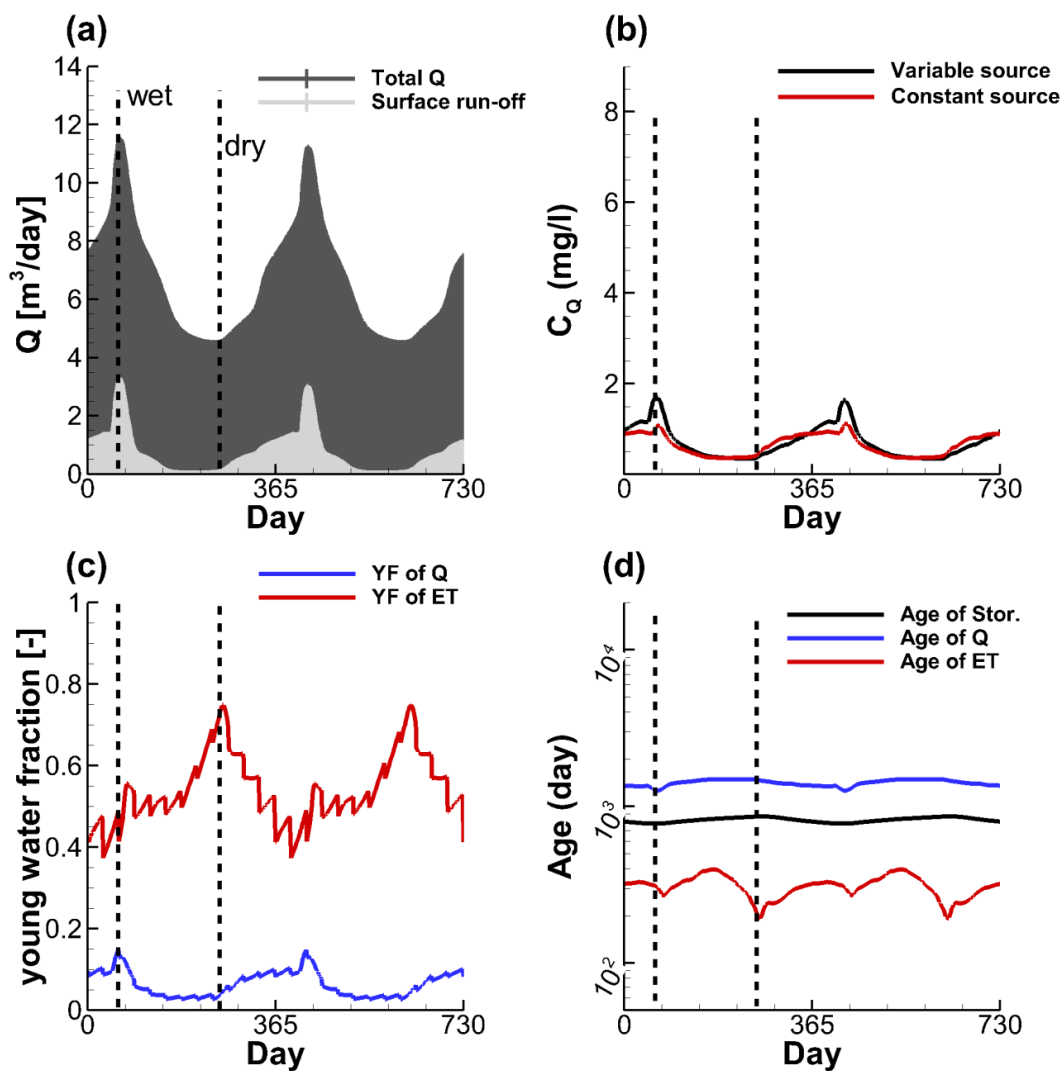
4 Results and discussion

290 For all the scenarios, the simulated Q, in-stream nitrate concentrations C_Q , the young water fractions YF , and the
water ages show seasonal fluctuations. Figure 3 shows these fluctuations for the cross-section with topographic slope
of 1:20. Q reaches its maximum towards the end of the wet winter in late February and reaches its minimum during
the drier late summer in mid-September. Total Q consists of a portion of groundwater discharge and a portion
generated via surface-runoff (Figure 3a). For C_Q , high concentrations are reached during the wet season and low
295 concentrations are reached during the dry season (Figure 3b). Figure 3c depicts opposing fluctuation patterns of YF_Q
and YF_{ET} . Young water in ET is low during the wet and high during the dry season, while young water in Q is low
during the dry and high during the wet season. ET generally has larger young water fractions than Q as ET has a higher
probability to remove young water from the shallow soil rather than the older water in the deeper aquifer. Especially
during the dry season, most precipitation can be quickly removed by ET. Figure 3d shows that ET age ranges from
300 192 to 395 days, being older during the wet and younger during the dry season. Simulated discharge age ranges from
1259 to 1490 days, being younger during the wet and older during the dry season.

Generally, the seasonal fluctuation patterns of C_Q , with both variable source and constant source, are highly correlated
with the fluctuation pattern of the YF_Q with Spearman rank-correlation coefficients of 0.81 and 0.93, respectively. The
calculated Da for streamflow is 13, demonstrating that the degradation time-scale is significantly shorter than the



305 transport time-scale. This means young streamflow is the main contributor of nitrate mass as most of the nitrate in the
 older water has been degraded before reaching the stream.



310 **Figure 3.** Simulated (a) Q , (b) in-stream nitrate concentration C_Q , (c) young water fractions YF_Q and YF_{ET} , and (d)
 water ages for the cross-sectional aquifer with topographic slope of 1:20.



4.1 In-stream nitrate level

With the help of our simulations, it is possible to systematically explore the influence of topographic slope on the concentrations of nitrate exported to the stream. For each scenario with time-variant nitrate source concentration, we analyzed the temporal mean C_Q , as well as the C_Q extracted at a wet time and a dry time (marked with the dashed line in Figure 3b).

Figure 4a shows that the mean C_Q responds to changes in topographic slope: (1) the mean C_Q increases when the topographic slope decreases from 1:20 to 1:60, (2) the mean C_Q drops sharply when the topographic slope further decreases to 1:100, and (3) the mean C_Q increases again when the topographic slope decreases from 1:100 to 1:1000. The maximum and minimum values are reached at topographic slopes of 1:60 and 1:100, respectively, rather than in the flattest or steepest landscapes. According to the distinct responses within different ranges of topographic slopes, we sorted the virtual catchments into three classes in terms of the mean topographic slopes of the aquifer (or the landscape) as follows (Figure 4a):

- C1, with topographic slope in the range [1:20 – 1:60]
- C2, with topographic slope in the range [1:60 – 1: 100]
- C3, with topographic slope in the range [1: 100 – 1: 1000]

A similar three-class response can be observed for the wet-time C_Q (blue line in Figure 4a), it is even more pronounced than the one for the mean C_Q . The dry-time C_Q decreases linearly from steeper to flatter landscapes, not exhibiting specific classes. The effect of topographic slope on C_Q is hence dominated by the wet season response as most of the discharge was produced during the wet season. The response pattern of the YF_Q is highly identical to the C_Q response patterns, also showing a three-class response (Figure 4b). This indicates that the topographic slope influences the C_Q levels via changing the young water fraction. Figure 4c demonstrates that the discharge age T_Q tends to be younger in steeper and older in flatter landscapes, especially during the dry season. This pattern did not show any correlation to the response of C_Q , thus suggesting that discharge age T_Q is not the most valuable predictor of C_Q .

335

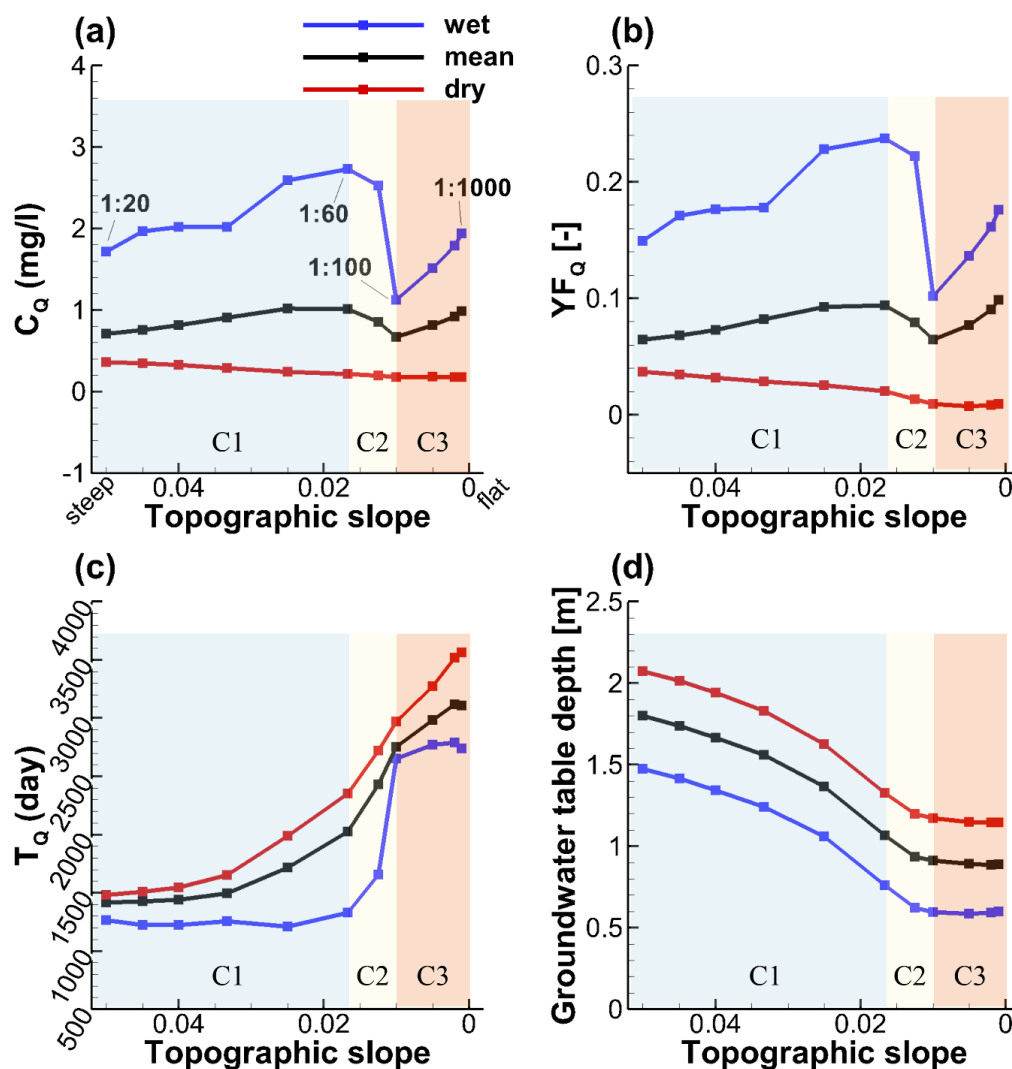


Figure 4. The simulated (a) in-stream concentration C_Q , (b) young water fraction in streamflow YF_Q , (c) discharge age T_Q , and (d) spatially-averaged depth of the groundwater table from the land surface, in relation to the topographic slope for the simulated cross-sections. The temporal mean, the dry time value and the wet time value of these variables were plotted. C1, C2 and C3 represent the landscape classes 1, 2, and 3, respectively.

340

Mechanistically interpreting the three-class response of the YF_Q to topographic slope requires a closer look at the flow processes in the cross-sections. We plotted the subsurface flow fields for the wet season for the cross-sections of slope 1:20, 1:60, 1:100, and 1:1000 (Figure 5).

345



(1) For C1 (slope 1:20 – 1:60), Figure 5a reveals that the hillslope part of the aquifer with a slope of 1:20 is largely unsaturated so that the flow paths in this area are characterized by vertical infiltration (Figure 5a). In contrast, the valley bottom is fully saturated. Overall, 34% of the subsurface domain (in volume) is characterized by vertical flow. For this scenario two main discharge routes to the stream can be identified: (i) A fraction of the groundwater flows through the fully saturated zone and exits the aquifer to the stream, and (ii) another fraction exits the aquifer via seepage near to where the groundwater table intersects the land surface, indicated by a large exchange flux (from subsurface to surface, positive). The seepage represents a preferential flow path allowing for rapid discharge via overland flow instead of slower discharge via the sub-surface with longer transit times. Reducing the topographic slope to 1:60 does not significantly change the flow pattern (Figure 5b). However, the spatially averaged depth of the groundwater table is reduced from 1.5 m to 0.8 m (Figure 4d). This change leads to two main effects: (i) the infiltration processes is weakened, indicated by the fact that the portion of subsurface domain characterized by vertical flow is reduced from 34% to 22%, and (ii) the shallow subsurface flow processes, such as seepage, are promoted, increasing the amount of water taking the short shallow flow paths in the system. This is proved by that the portion of streamflow generated by surface run-off increased from 3.2 m³/day to 7.1 m³/day (Figure 5a, b).

Subsequently, the contribution of young water to streamflow significantly increases when the slope decreases from 1:20 to 1:60, also supported by the computed TTDs (Figure 6a). Given that the groundwater storage significantly increases with decreasing slope, this effect is similar to the “inverse storage effect” that has been described in *Harman*, [2015] as the relative contribution of young water to stream flow increasing with increasing storage. *Kim et al.*, [2016] also reported based on their lysimeter experiments that younger water was discharged in greater proportion under wetter conditions compared to drier conditions. However, the observed changes in groundwater table depth (thus storage) in our study were caused by topography rather than by climate.

(2) For C2 (slope 1:60 – 1:100), even though the groundwater table depth is still decreasing with decreasing slope, the flow pattern experiences a rapid change. The seepage flow vanishes because the groundwater table (fully or partially) disconnects from the land surface (Figure 5c). The water that would have flown to the stream via seepage has to take slower flow paths in the subsurface to the valley bottom. The surface run-off dropped significantly from 7.1 m³/day to 0.5 m³/day (Figure 5c, d). Basically, decreasing the topographic slope reduces the horizontal component of the hydraulic head gradients, which is obvious as part of the precipitation falls at lower elevations instead of farther up the hillslope. The reduced head gradient generally slows down the groundwater flow velocity.

Several hydrologic studies have described two different flow systems in aquifers: (i) a recharge-limited system where the thickness of the unsaturated zone is sufficient to accommodate any water-table rise and thus the elevation of the groundwater table is limited by the recharge, and (ii) a topography-limited system where the groundwater table is close or connected to the land surface such that any fluctuation in groundwater table can result in considerable change in surface runoff [*Werner and Simmons*, 2009; *Michael et al.*, 2013]. In our study, the aquifer of C1 is a partially topography-limited system (e.g. Figure 5a, b) (the hillslope is recharge-limited while the valley bottom is topography-limited). In C2 the aquifer is transformed into a fully recharge-limited system (from Figure 5b to 5c) due to the reduced



hydraulic head gradients. This transformation switches off the preferential flow paths via seepage to the land surface and significantly reduces the YF_Q .

(3) For C3 (slope 1:100 – 1:1000), the aquifer is fully recharge-limited without any preferential flow via land surface. Further reducing the topographic slope to 1:1000 mainly changes the spatial distribution of the unsaturated zone
385 (comparing Figure 5d with 5c). Because the groundwater table depth (thus the storage) more or less remains unchanged (Figure 4d), interestingly, here the “inverse storage effect” does not apply anymore and cannot explain the increase of the YF_Q when the topography becomes flatter.

However, on flatter landscapes, local flow cells are more likely to form, where water infiltrates to the aquifer and eventually exits the aquifer via ET rather than via flow to the stream (Figure 5d, the local flow cells are more
390 pronounced in the dry season, see Figure S1d in the supporting information). Simply put, precipitation falling farther from the stream has a lower chance to reach the stream and a higher chance to be intercepted by ET on its way to the stream, because the flow velocity is much lower due to the smaller horizontal component of hydraulic head gradient. While precipitation water close to the stream has a higher chance to contribute to streamflow. We hypothesize that the increase of the YF_Q , as indicated by the computed TTDs (Figure 6b), is due to this reduction of the longer flow paths
395 and the persistence of shorter flow paths.

To further verify our hypothesis, we mapped the land area contributing to the streamflow (streamflow generation zone) using a particle tracking algorithm in HydroGeoSphere [Yang *et al.*, 2018]. Figure 7 demonstrates the streamflow generation zone in February for the slope 1:100 and 1:1000, respectively. For the aquifer with a slope of 1:100, the zone extends further into the hillslope, with relatively younger streamflow generated close to the stream and old
400 streamflow (i.e. age > 5 years) generated further up the hillslope. When the slope is reduced to 1:1000, the streamflow generation zone is much closer to the stream. The hillslope that used to generate old streamflow does not contribute to streamflow anymore. This means that in flatter landscapes, the evolution of local flow cells reduces the connectivity between the stream and the more distant hillslopes by intercepting the longer flow paths at the land surface before they can reach the stream (Figure 7b), leading to an increase in the YF_Q . We refer to this as the “local flow cells effect”.

405

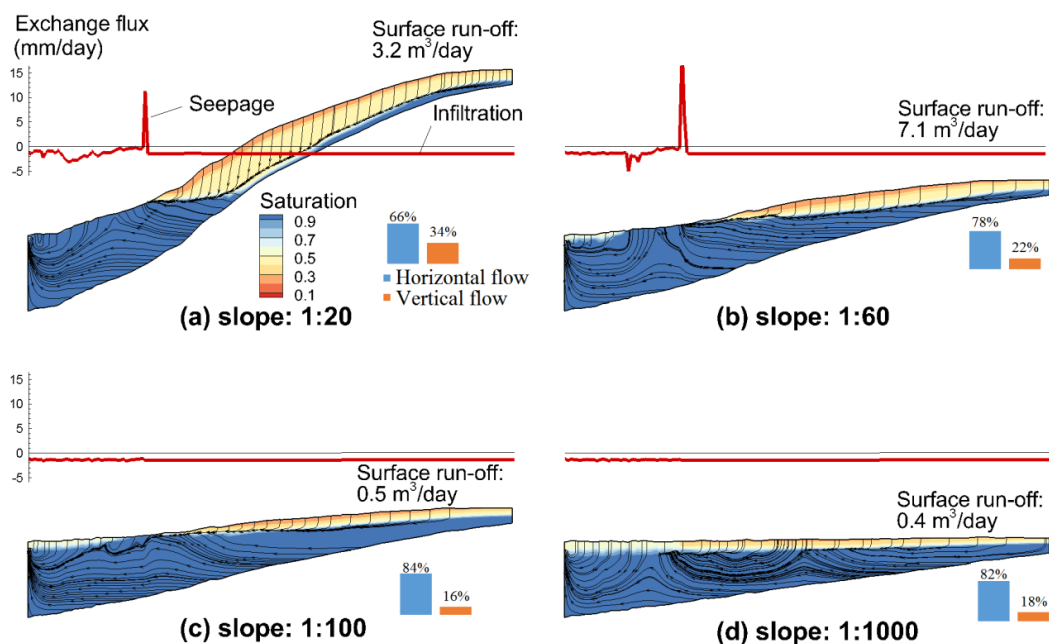
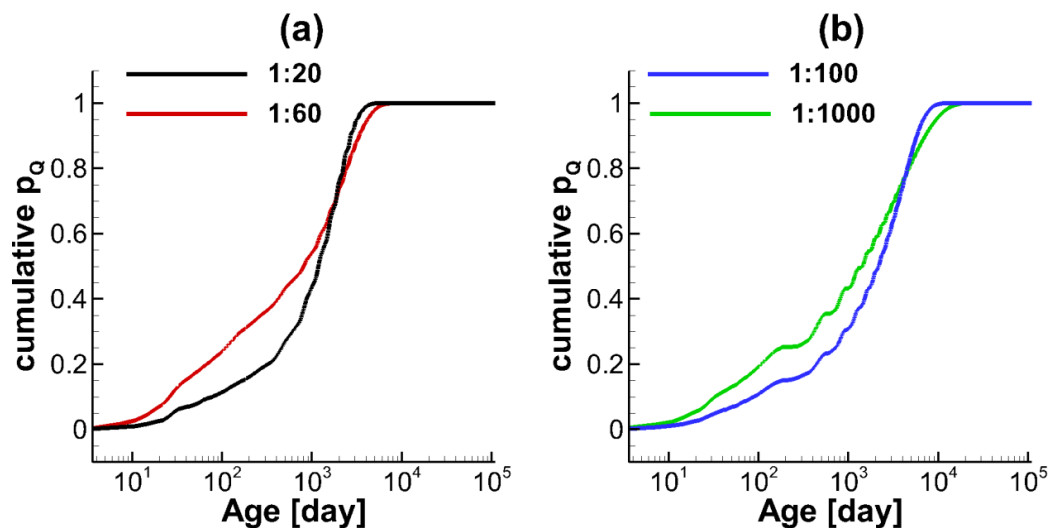
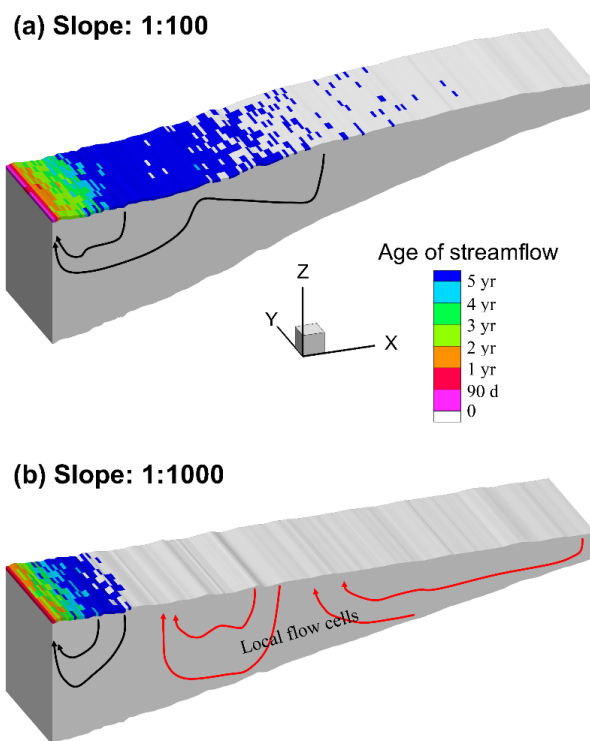


Figure 5. The distribution of saturation, flow paths, and exchange fluxes between the surface and the subsurface in the wet season (February) for the aquifer with topographic slope (a) 1:20, (b) 1:60, (c) 1:100, and (d) 1:1000. The black lines represent the flow paths. The red curves show exchange fluxes (along the cross-sectional profiles), positive values indicate seepage to the land surface and negative values indicate infiltration to the subsurface.





415 **Figure 6.** The computed cumulative TTDs for Q during the wet season (February), for the cross-sections with topographic slope of (a) 1:20 and 1:60, and (b) 1:100 and 1:1000.



420 **Figure 7.** Maps showing the land areas that contribute to streamflow via subsurface flow through the aquifer with topographic slopes of (a) 1:100 and (b) 1:1000. The color indicates the age of the streamflow. Black lines indicate the flow paths to the stream, and red lines indicate the local flow cells that are not connected to stream.

425 In summary, we identified three classes for the response of in-stream concentrations to topographic slope under a humid climate. When the landscape becomes flatter, the hydraulic head gradient as the main driving force, changes the aquifer from a partially topography-limited system with preferential overland flow (C1) to a recharge-limited system that is more likely to form local flow cells (C3). For the aquifer of C2, which is a transitional class between C1 and C3, YF_Q and nitrate concentrations experience a sharp drop once the preferential overland flow paths cannot be maintained. For the aquifer of C1 (or C3), decreasing slopes tend to generate a higher fraction of young streamflow and export nitrate at higher concentrations. However, the former is dominated by the “inverse storage effect” while



430 the latter is dominated by the “local flow cells effect”. In this sense, the response of in-stream concentrations to topographic slope is threshold-like rather than monotonous.

4.2 In-stream nitrate seasonal variations

435 Simulated results demonstrate significant seasonal variations of C_Q for all the scenarios (Figure S2 in the supporting information). Basically, this variation in C_Q is caused either by the fluctuation of the nitrate source input, or by fluctuations in degradation time associated with the varying transit times. The calculated source contribution for our simulated scenarios indicates that only 2 to 33 % of the variation of C_Q can be attributed to the fluctuation of source concentrations (Figure 8a). This means that the nitrate concentration fluctuations in all simulated cross-sections are dominated by the variability in degradation time (transit time). In other words, significant seasonal variation of the
440 nitrate concentration in streamflow can be expected under the considered humid climate even when nitrate is applied to the aquifer in a constant manner without any variation. These seasonal fluctuations of transit time and C_Q were frequently explained using the “inverse storage effect” [Harman, 2015; Yang *et al.* 2018]: during the wet season Q has a strong preference for young water associated with higher concentrations, which would not occur during dry periods due to the deactivation of the shallow fast flow processes. This effect was revealed in the computed TTDs for
445 Q indicated by the shift between wet and dry seasons (Figure S3 in the supporting information).

The response of the source contributions to topographic slope is threshold-like (Figure 8a): the source contributions in C1 were significantly higher than the ones in C3. Especially for the landscapes of C3, the fluctuation of C_Q was hardly impacted by source variability. Mechanically, the seasonal source fluctuation is more likely to be damped by relatively longer transit times in C3 landscapes, which are relatively flat.

450 Given that the seasonal C_Q variation can be attributed more to the variation in transit times (thus to the variation in the YF_Q), it was expected that the standard deviations of C_Q and YF_Q (Figure 8b, c) had similar responses to the topographic slope. Both of the responses exhibit a threshold-like pattern, similar to the response of the mean C_Q (Figure 4a). This is because C_Q during the dry season is generally low, regardless of whether the landscape is steeper or flatter. The overall response of $\sigma(C_Q)$ to topographic slope is determined by the response of the relatively high C_Q during the wet season, and can be interpreted in the same three-class pattern: $\sigma(C_Q)$ increases with the decrease of slope within C1
455 (or C3), suggesting that flatter landscapes tend to export nitrate with more seasonal fluctuations in C_Q for C1 (or C3). However, for C2, a significant drop in this fluctuation can be expected when the landscape transforms from C1 to C3. As a result, the maximum seasonal variation was reached at the slope of 1:60. For the mechanistic interpretation please refer to section 4.1.

460

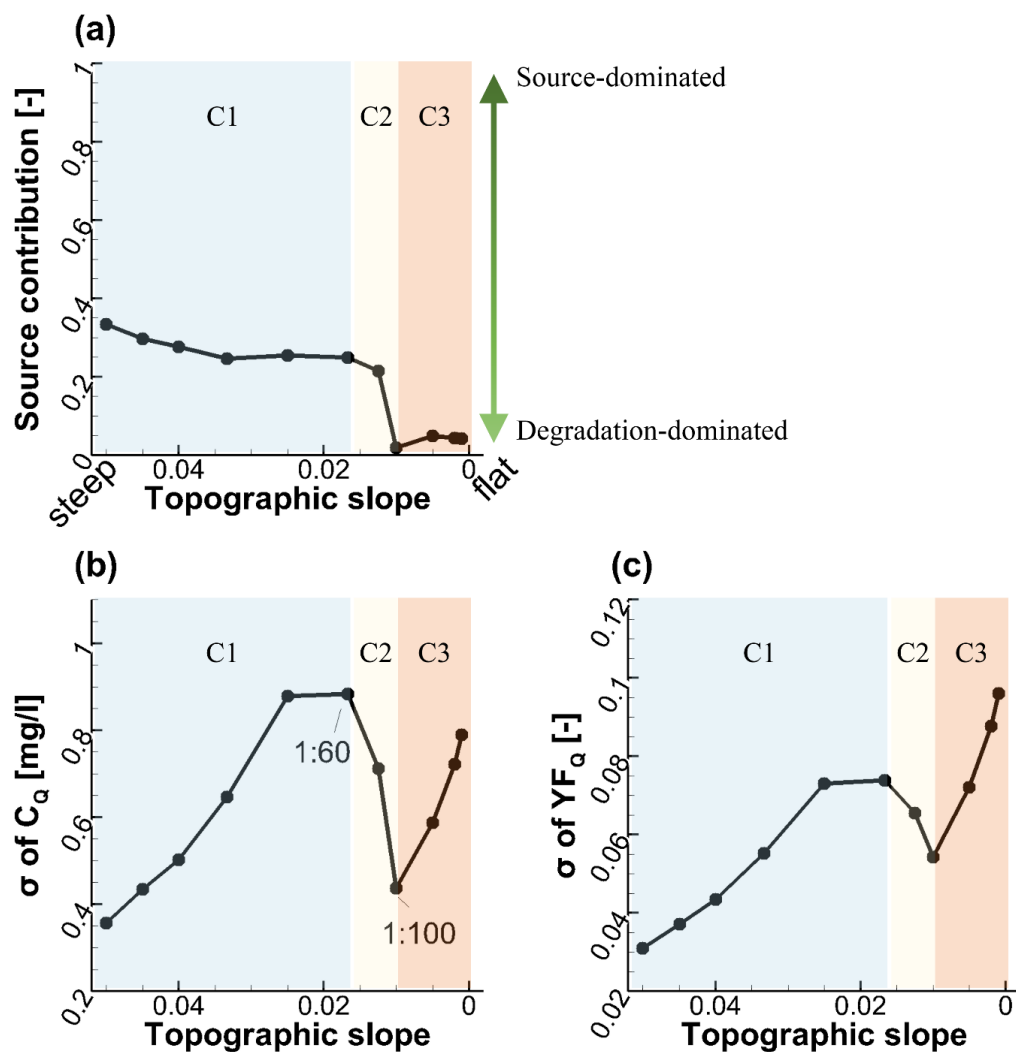


Figure 8. The calculated (a) source contribution to the variation of in-stream concentration C_q , (b) σ of C_q , (c) σ of YF_q . C1, C2 and C3 represent for the landscape classes 1, 2, and 3, respectively.

465

4.3 Discussion

Jasechko et al., [2016] reported that (the logarithm of) catchment topographic slope was significantly negatively correlated with young streamflow fractions with a spearman rank correlation of -0.36. This conclusion was made statistically based on their observed 254 sites. Our numerical study based on the eleven cross-sectional aquifers with different slopes but identical climate conditions resulted in more physically-based information that goes beyond such statistical correlations. Our results show that young streamflow fraction and slope possess a threshold-like three-class

470



relation instead of a monotonous relation. The negative correlation between slope and young streamflow fraction can be found in slope classes C1 and C3, but not in the slope class C2.

475 For the landscapes of the C1 class, catchments are likely to form a partially topography-limited flow system with preferential flow paths due to the relatively high hydraulic gradient. Groundwater storage is larger when the landscape becomes flatter. The “inverse storage effect” explains the increases of young streamflow in flatter landscapes during the wet season. This is consistent with the statement made by *Jasechko et al.*, [2016] as the young streamflow fraction is more prevalent in flatter catchments which are characterized by more shallow lateral flow and less vertical infiltration. This phenomenon is also consistent with a negative correlation between groundwater table depth and
480 young streamflow fraction, which has been frequently reported [*Bishop et al.*, 2004; *Seibert et al.*, 2009; *Frei et al.*, 2010; *Jasechko et al.*, 2016]. For landscapes of the C3 class, the negative correlation between young streamflow fraction and slope was also confirmed. However, here, the “inverse storage effect” fails to explain this correlation because neither the groundwater storage nor the groundwater table depth undergo any significant change. Our study points at the formation of local flow cells that do not reach the stream causing the increase of young streamflow
485 fraction. This phenomenon has not yet been reported to the best of our knowledge. However, for landscapes of the C2 class, our results suggest that young streamflow can be more prevalent in steeper landscapes with active preferential overland flow paths than in flatter landscapes with the fast preferential flow paths deactivated. This trend violates the otherwise negative correlation between topographic slope and young streamflow fraction. In this sense, the negative correlation between catchment topographic slope and young streamflow fraction is not conclusive.

490 Basically, the position of the groundwater table, flow path lengths and flow velocities, which are all different for different topographic slopes, jointly affect the young streamflow fractions and nitrate export concentrations. Besides that, temporal variability of these three factors drives the distinct responses of the young streamflow fraction to topographic slope between seasons. For example, the three-class response is more pronounced in the wet winter than in the dry summer. This demonstrates that the system is complex and apparently contains various threshold effects
495 disturbing a straightforward monotonous relationship between any catchment characteristics (e.g. slope) and young water fraction (or streamflow concentration). In this sense, systematically investigating the reaction of the flow dynamics to catchment characteristic is necessary, rather than assuming a straightforward cause-effect relationship that can be misleading.

500 Our results demonstrate that stream water quality is more vulnerable in flatter landscapes when the compared catchments have consistent flow patterns (e.g., both are C1 or C3 aquifers). The results also highlight the importance of fast preferential flow on exporting the young water and nitrate. In mountainous central German catchments, these groundwater seepages to the land surface can be frequently observed. They can be identified as “hot spots” allowing for the export of nutrients with higher concentrations. This suggests that more attention should be paid to catchments with “hot spots” concerning the management of stream water quality and agricultural activity.

505 Concerning the seasonal variations of nitrate export, our results showed that the high peak concentrations occurred in the wet and the low in the dry seasons, being consistent with the findings of previous studies [*Benettin et al.* 2015; *Harman*, 2015; *Kim et al.*, 2016; *Yang et al.*, 2018]. The lowest concentrations were hardly affected by topographic



slope, therefore the magnitude of seasonal variations depended on how high the C_Q rises during the wet seasons. This indicates that, for similar catchments in temperate humid climates, a high mean in-stream concentration level also
510 means a high seasonal variation. The source contribution to seasonal variations is higher for C1 landscapes (> 0.2) than for C3 landscapes (almost zero). This implies that changes in the nitrate source input due to, e.g., changing crop type, land use or fertilizer application amount, are more likely to cause a detectable short-term (e.g. seasonal) response of the in-stream concentration for mountainous catchments. For flat landscapes, this response would be weaker.

515 **4.4 Limitations and outlook**

The cross-comparison between cross-sectional aquifers with differing topographic slopes provides physically-based insights into the effects of slope on nitrate export responses in terms of mean concentration level and seasonal variations. However, this study is limited in scope in that it neglects other factors that may also have important impacts on the young streamflow and nitrate export processes:

520 First, the modeled cross-sectional aquifers were unconfined with an impermeable base and prescribed heterogeneity. Our model conclusions may be limited to the regional scale. Other catchment characteristics such as landscape aspect, catchment area, aquifer permeability or drainage ability, aquifer depth, stream bed elevation and fractured bedrock permeability can potentially change the flow patterns and age composition in streamflow [McGlynn *et al.*, 2003; Broxton *et al.*, 2009; Sayama and McDonnell, 2009; Stewart *et al.*, 2010; Jasechko *et al.*, 2016; Heidbüchel *et al.*,
525 2013, 2020]. For example, aquifers with high permeability or highly fractured bed rock are more likely to use deep rather than shallow flow paths and preferential discharge routes that lead to rapid drainage. Apart from that, it was reported that hydrological features such as precipitation variability, ET, antecedent soil moisture are also significantly linked to transit times [Sprenger *et al.*, 2016; Wilusz *et al.* 2017; Evaristo *et al.*, 2019; Heidbüchel *et al.*, 2013, 2020]. For example, compared to uniform precipitation, event-scale precipitation is more likely to trigger rapid surface runoff
530 and intermediate flow, such that the contribution of young water from storage to streamflow can be increased. Therefore, further research should consider a more complex model structure involving various heterogeneity and climate types.

Second, several main simplifications were used in the formulation of nitrate transport processes. (i) Transport modelling employed a constant degradation rate coefficient assuming that transit time was the only factor to determine
535 degradation. This assumption neglected other factors that can spatially and temporally affect denitrification rates, such as temperature, redox boundaries (e.g., high oxygen concentration in shallow flow paths), amount of other nutrients (e.g. carbon), which also contribute to the seasonality in nitrate concentrations [Böhlke *et al.*, 2007]. Apart from that, we did not account for the long-term (decades [Van Meter *et al.*, 2017]) nitrate legacy effect as the dissolved nitrate in groundwater reservoirs degraded continuously in our model, which would not occur in older reservoirs where the denitrification is very slow or deactivated (e.g. due to the lack of carbon source). (ii) In our simulations, the
540 complexities of the nitrogen pool were simplified by integrally defining a source concentration curve. The variability of the source input was implicitly considered by forcing the source concentration to vary along that curve over the course of a year. The accurate simulation of C_Q would depend on a realistic estimation of the input source curve.



545 However, it is not that important in our study as we were focused on understanding how the response changes with
regard to topographic slope rather than on accurately reproducing C_Q . (iii) The nitrate source was uniformly applied
across the land surface in our modelling. However, strong source heterogeneity may exist in catchments. For example,
the source concentrations vary between land uses or along the soil profile [Zhi *et al.*, 2019]. This spatial source
heterogeneity could affect the seasonal variations of C_Q [Musolff *et al.*, 2017; Zhi *et al.*, 2019] and should be considered
in further research.

550 Despite these limitations, the numerical experiments in this study could clearly identify a three-class response of young
streamflow and nitrate export to topographic slope under a humid seasonal climate, and show that hydraulic gradient
is an important factor causing the differences between the classes. This was achieved by using the advantages of a
physically-based flow simulation that allows for a more mechanistic evaluation of flow processes, which would be
impossible with a purely data driven analysis based on, e.g., isotopic tracers only.

555

5 Conclusions

Previous data driven studies suggested that catchment topographic slope impacts age composition of streamflow and
consequently the in-stream concentrations [Jasechko *et al.*, 2016]. We attempted to find more mechanistic
explanations for these effects. We chose a cross-section from the small agricultural catchment ‘Schäferfetal’ in Central
560 Germany and generated eleven synthetic cross-sections of varying topographic slope. The groundwater and overland
flow, and the nitrate transport in these cross-sections were simulated using a coupled surface-subsurface model. Water
age compositions for Q and ET were determined using numerical tracer experiments. Based on the calculated flow
patterns, in-stream nitrate concentration C_Q and young water fractions in streamflow YF_Q , we systematically assessed
the effects of varying catchment topographic slopes on the nitrate export dynamics in terms of the concentration level
565 (annual mean) and its seasonal variability. The main conclusions of this study are:

- Under the considered humid climate, C_Q is related to topographic slope by a three-class response. When the
landscape becomes flatter, the hydraulic head gradient is the main driving force, changing the aquifer from a
partially topography-limited system with preferential overland flow (C1) to a recharge-limited system that is
more likely to form local flow cells (C3). For landscapes falling into the classes C1 or C3, flatter landscapes
570 tend to generate more young streamflow and export nitrate of higher C_Q . However, for the former this is due
to the “inverse storage effect” and for the latter this is due to the “local flow cells effect”. For the transitional
class C2, YF_Q and nitrate concentration decrease sharply once the flatter landscapes are no longer able to
maintain the fast preferential overland flow paths.
- For catchments in temperate humid climates with considerable seasonality in wetness conditions, the seasonal
575 variation of C_Q is dominated by the variability in transit times and in turn degradation, rather than by the
variability in the nitrate source. Especially for the aquifer of the C3 class, significant seasonal variation of C_Q
can be generated even without any variability in the nitrate source.



- The response of the seasonal variation of C_Q to topographic slope is similar to the one of the mean C_Q . For the landscapes of the C1 or C3 classes, seasonal variation tends to be more pronounced for flatter landscapes. However, for the C2 class, a significant decrease in this variation can be expected when fast preferential overland flow paths are switched off on flatter landscapes.

580

Overall, this study provides a mechanistic perspective on how catchment topographic slope affects nitrate export patterns. The use of a fully-coupled flow and transport model extends the approach to investigate the effects of catchment characteristics beyond the frequently used tracer data-driven analysis. It can be used for similar studies of other catchment characteristics and for other solutes. The results of this study reveal potential implications for the management of stream water quality and agricultural activity, in particular for catchments in temperate humid climates with pronounced seasonality. Given the limitations of this study, future work should be devoted to improve the degradation formulation, to investigate further catchment characteristics, as well as to consider various climate types.

585

590 Notation

	t	[T] time
	T	[T] age / transit time / residence time
	J	[LT^{-1}] precipitation
	ET	[LT^{-1}] evapotranspiration
595	Q	[LT^{-1}] discharge / streamflow
	ps	[-] age distribution of storage
	$p_{ET/Q}$	[-] age distribution for evapotranspiration / discharge, equivalent to TTD
	C	[ML^{-3}] concentration
	C_j	[ML^{-3}] source concentration
600	C_Q	[ML^{-3}] in-stream solute (nitrate) concentration
	T_Q	[ML^{-3}] age (transit time) of discharge
	Da	[-] Damköhler number
	YF_Q	[-] young water fraction in streamflow, or young streamflow fraction
	YF_{ET}	[-] young water fraction in ET

605

Code/Data availability

All data used in this study are listed in the supporting information and uploaded separately to HydroShare [Yang, 2020].



610 **Author contributions**

JY: conceptualization, methodology, software, formal analysis, visualization, writing - review & editing; IH: writing - review & editing; CL: conceptualization, methodology, review & editing; YX: methodology; AM: conceptualization; JF: conceptualization, review & editing.

615 **Competing interests**

The authors declare that they have no conflict of interest.

Acknowledgments

This research was supported by the National Natural Science Foundation of China (No. 52009032), and the
620 Fundamental Research Funds for the Central Universities (No. B210202019).

References

- Anis, M. R., & Rode, M. (2015). Effect of climate change on overland flow generation: A case study in central Germany. *Hydrological Processes*, 29(11), 2478–2490.
- 625 Benettin, P., Y. van der Velde, S. E. A. T. M. van der Zee, A. Rinaldo, and G. Botter (2013), Chloride circulation in a lowland catchment and the formulation of transport by travel time distributions, *Water Resources Research*, 49(8), 4619–4632, doi: 10.1002/wrcr.20309.
- Benettin, P., J. W. Kirchner, A. Rinaldo, and G. Botter (2015), Modeling chloride transport using travel time distributions at plynlimon, wales, *Water Resources Research*, 51(5), 3259–3276, doi:10.1002/2014WR016600.
- 630 Bishop, K., Seibert, J., Köhler, S. and Laudon, H. (2004), Resolving the Double Paradox of rapidly mobilized old water with highly variable responses in runoff chemistry. *Hydrol. Process.*, 18: 185-189. <https://doi.org/10.1002/hyp.5209>
- Böhlke, J. K., M. E O’Connell, and K. L Prestegard (2007), Ground water stratification and delivery of nitrate to an incised stream under varying flow conditions, *Journal of environmental quality*, 36, 664–80,
635 doi:10.2134/jeq2006.0084.
- Broxton, P. D., P. A. Troch, and S. W. Lyon (2009), On the role of aspect to quantify water transit times in small mountainous catchments, *Water Resour. Res.*, 45, W08427, doi:10.1029/2008WR007438.
- Dupas, R., A. Musolff, J. W. Jawitz, P. S. C. Rao, C. G. Jäger, J. H. Fleckenstein, M. Rode, and D. Borchardt (2017), Carbon and nutrient export regimes from headwater catchments to downstream reaches, *Biogeosciences*, 14(18),
640 4391–4407, doi:10.5194/bg-14-4391-2017.
- Evaristo, J., Kim, M., van Haren, J., Pangle, L. A., Harman, C. J., Troch, P. A., & McDonnell, J. J. (2019). Characterizing the fluxes and age distribution of soil water, plant water, and deep percolation in a model tropical ecosystem. *Water Resources Research*, 55(4), 3307-3327.



- 645 Frei, S., Lischeid, G. and Fleckenstein J.H. (2010) Effects of micro-topography on surface-subsurface exchange and runoff generation in a virtual riparian wetland – a modeling study, *Advances in Water Resources*, 33(11):1388-1401.
- Harman, C. J. (2015), Time-variable transit time distributions and transport: Theory and application to storage-dependent transport of chloride in a watershed, *Water Resources Research*, 51(1), 1–30, doi:10.1002/2014WR015707.
- Harman, C. J. (2019). Age-Ranked Storage-Discharge Relations: A Unified Description of Spatially Lumped Flow and Water Age in Hydrologic Systems. *Water Resources Research*, 55(8), 7143-7165.
- 650 Heidebüchel, I., P. A. Troch, and S. W. Lyon (2013). Separating physical and meteorological controls of variable transit times in zero-order catchments. *Water Resources Research*, 49, 7644–7657, doi:10.1002/2012WR013149.
- Heidebüchel, I., J. Yang, A. Musolff, P. Troch, T. Ferré J. H. Fleckenstein (2020). On the shape of forward transit time distributions in low-order catchments. *Hydrology and Earth System Sciences*, doi: 10.5194/hess-2019-440.
- Hrachowitz, M., O. Fovet, L. Ruiz, and H. H. G. Savenije (2015), Transit time distributions, legacy contamination and variability in biogeochemical 1/f scaling: how are hydrological response dynamics linked to water quality at the catchment scale?, *Hydrological Processes*, 29(25), 5241–5256, doi:10.1002/hyp.10546.
- 655 Hrachowitz, M., P. Benettin, B. M. Van Breukelen, O. Fovet, N. J. Howden, L. Ruiz, Y. Van Der Velde, and A. J. Wade (2016), Transit times-the link between hydrology and water quality at the catchment scale, *Wiley Interdisciplinary Reviews: Water*, 3(5), 629–657.
- 660 Jasechko, S., Kirchner, J., Welker, J. et al. Substantial proportion of global streamflow less than three months old. *Nature Geosci* 9, 126–129 (2016). <https://doi.org/10.1038/ngeo2636>
- Kaandorp, V. P., Louw, P. G. B., Velde, Y., & Broers, H. P. (2018). Transient Groundwater Travel Time Distributions and Age - Ranked Storage - Discharge Relationships of Three Lowland Catchments. *Water Resources Research*, 54, 4519– 4536. <https://doi.org/10.1029/2017WR022461>
- 665 Kim, M., L. A. Pangle, C. Cardoso, M. Lora, T. H. Volkmann, Y. Wang, C. J. Harman, and P. A. Troch (2016), Transit time distributions and storage selection functions in a sloping soil lysimeter with time-varying flow paths: Direct observation of internal and external transport variability, *Water Resources Research*, 52(9), 7105–7129.
- Li, Y., Chen, Y., Li, Z., 2019. Dry/wet pattern changes in global dryland areas over the past six decades. *Glob. Planet. Chang.* 178, 184–192. <https://doi.org/10.1016/j.gloplacha.2019.04.017>.
- 670 McGlynn, B., J. McDonnell, M. Stewart, and J. Seibert (2003), On the relationships between catchment scale and streamwater mean residence time, *Hydrol. Processes*, 17, 175– 181, doi:10.1002/hyp.5085.
- Michael, H.A., Russoniello, C.J., Byron, L.A., 2013. Global assessment of vulnerability to sea-level rise in topography-limited and recharge-limited coastal groundwater systems. *Water Resour. Res.* 49, 1–13.
- Musolff, A., C. Schmidt, B. Selle, and J. H. Fleckenstein (2015), Catchment controls on solute export, *Advances in*
- 675 *Water Resources*, 86, 133–146.
- Musolff, A., J. H. Fleckenstein, P. S. C. Rao, and J. W. Jawitz (2017), Emergent archetype patterns of coupled hydrologic and biogeochemical responses in catchments, *Geophysical Research Letters*, 44(9), 4143–4151, doi:10.1002/2017GL072630.



- 680 Nguyen, T. V., Kumar, R., Lutz, S. R., Musolff, A., Yang, J., & Fleckenstein, J. H. (2021). Modeling nitrate export from a mesoscale catchment using storage selection functions. *Water Resources Research*, 57, e2020WR028490. <https://doi.org/10.1029/2020WR028490>
- Oldham, C. E., D. E. Farrow, and S. Peiffer (2013), A generalized damköhler number for classifying material processing in hydrological systems, *Hydrology and Earth System Sciences*, 17(3), 1133–1148, doi:10.5194/hess-17-1133-2013.
- 685 Rinaldo, A., P. Benettin, C. J. Harman, M. Hrachowitz, K. J. McGuire, Y. Van Der Velde, E. Bertuzzo, and G. Botter (2015), Storage selection functions: A coherent framework for quantifying how catchments store and release water and solutes, *Water Resources Research*, 51(6), 4840–4847.
- Rodriguez, N. B., McGuire, K. J., & Klaus, J. (2018), Time-varying storage-water age relationships in a catchment with a mediterranean climate. *Water Resources Research*, 54(6), 3988-4008.
- 690 Sayama, T. & McDonnell, J. J. (2009), A new time-space accounting scheme to predict stream water residence time and hydrograph source components at the watershed scale. *Wat. Resour. Res.* 45, W07401.
- Seibert, J., Grabs, T., Köhler, S., Laudon, H., Winterdahl, M., and Bishop, K.: Linking soil- and stream-water chemistry based on a Riparian Flow-Concentration Integration Model, *Hydrol. Earth Syst. Sci.*, 13, 2287–2297, <https://doi.org/10.5194/hess-13-2287-2009>, 2009.
- 695 Sprenger, M., Seeger, S., Blume, T., & Weiler, M. (2016), Travel times in the vadose zone: Variability in space and time. *Water Resources Research*, 52, 5727-5754.
- Therrien, R., McLaren, Sudicky, R. E., & Panday, S. (2010). *Hydrogeosphere: A three-dimensional numerical model describing fully-integrated subsurface and surface flow and solute transport*, Groundwater Simulations Group. Waterloo, ON: University of Waterloo.
- 700 Stewart, M. K., Morgenstern, U. & McDonnell, J. J. (2010), Truncation of stream residence time: how the use of stable isotopes has skewed our concept of streamwater age and origin. *Hydrol. Process.* 24, 1646-1659.
- van der Velde, Y., G. De Rooij, J. Rozemeijer, F. Van Geer, and H. Broers (2010), Nitrate response of a lowland catchment: On the relation between stream concentration and travel time distribution dynamics, *Water Resources Research*, 46(11).
- 705 van der Velde, Y., P. J. J. F. Torfs, S. E. A. T. M. van der Zee, and R. Uijlenhoet (2012), Quantifying catchment-scale mixing and its effect on time-varying travel time distributions, *Water Resources Research*, 48(6), n/a–n/a, doi:10.1029/2011WR011310, w06536.
- Van Meter, K. J., N. B. Basu, and P. Van Cappellen (2017), Two centuries of nitrogen dynamics: Legacy sources and sinks in the mississippi and susquehanna river basins, *Global Biogeochemical Cycles*, 31(1), 2–23, doi:10.1002/2016GB005498.
- 710 Werner, A. D., and C. T. Simmons (2009), Impact of sea-level rise on seawater intrusion in coastal aquifers, *Ground Water*, 47, 197-204.
- Wilusz, D. C., Harman, C. J., & Ball, W. P. (2017). Sensitivity of catchment transit times to rainfall variability under present and future climates. *Water Resources Research*, 53(12), 10231-10256.



- 715 Yang, J., I. Heidbüchel, A. Musolff, F. Reinstorf, and J. H. Fleckenstein (2018), Exploring the dynamics of transit times and subsurface mixing in a small agricultural catchment, *Water Resources Research*, 54(3), 2317–2335, doi:10.1002/2017WR021896.
Yang, J. (2020). DS2020-2YJ, HydroShare, <http://www.hydroshare.org/resource/e266298e55834617a26242f6af9687e1>
- 720 Zhi, W., L. Li, W. Dong, W. Brown, J. Kaye, C. Steefel, and K. H. Williams (2019), Distinct source water chemistry shapes contrasting concentration-discharge patterns, *Water Resources Research*, 55(5), 4233–4251, doi:10.1029/2018WR024257.